Chemistry & Biology, Vol. 10, 655–662, July, 2003, ©2003 Elsevier Science Ltd. All rights reserved. DOI 10.1016/S1074-5521(03)00145-5

A Versatile tRNA Aminoacylation Catalyst Based on RNA

Hiroshi Murakami,[1,2] Hirohide Saito,[1,3] and Hiroaki Suga[1,*]
[1]Department of Chemistry
State University of New York, Buffalo
Buffalo, New York 14260

Summary

Aminoacyl-tRNA synthetase (ARS) ribozymes have potential to develop a novel genetic coding system. Although we have previously isolated such a ribozyme that recognizes aromatic amino acids, it could not be used as a versatile catalyst due to its limited ability of aminoacylation to a particular tRNA used for the selection. To overcome this limitation, we used a combination of evolutionary and engineering approaches to generate an optimized ribozyme. The ribozyme, consisting of 45 nucleotides, displays a broad spectrum of activity toward various tRNAs. Most significantly, this ribozyme is able to exhibit multiple turnover activity and charge parasubstituted Phe analogs onto an engineered suppressor tRNA ($tRNA^{Asn}_{CCCG}$). Thus, it provides a useful and flexible tool for the custom synthesis of mischarged tRNAs with natural and nonnatural amino acids.

Introduction

The X-ray structure of the large subunit of ribosome has revealed that its catalytic core resides in ribosomal RNA, not proteins [1–4]. This observation has not only provided conclusive evidence that ribosome is a ribozyme, but has also given strong support that the primitive translation system could have consisted of RNA molecules alone [5–16]. Aminoacyl-tRNAs play an exclusive role in decoding the genetic sequence on mRNA, and therefore a set of these molecules is also an essential component of the translation system. Aminoacylation of tRNA, which is the event that assigns the genetic triplet to each amino acid, is catalyzed by a set of enzymes called aminoacyl-tRNA synthetases (ARSs). Although in the present biological system ARSs are protein catalysts, the synthetases in the predated translation system could have also been RNA catalysts [17, 18].

Our laboratory has undertaken projects to generate such ARS ribozymes by means of in vitro selection and reported several ribozymes with analogous functions to ARS [13, 16, 19–21]. One of these ribozymes was generated based on the idea that a 5′ leader sequence of precursor tRNA could have catalyzed aminoacylation [16]. We succeeded in evolving a catalytic precursor tRNA (pre-24), in which the 5′ leader sequence selectively charges aromatic amino acids, such as phenylalanine (Phe) and tyrosine (Tyr), to the 3′ end of tRNA [22]. We have also shown that M1 RNA can cleave the 5′ leader portion from the tRNA sequence; this catalytic segment, referred to as r24, is able to charge the amino acids onto the mature tRNA in *trans* (Figure 1A). Thus, this *trans*-acting ribozyme exhibits the analogous function of ARSs.

More recently, we have begun investigating technological applications for this ribozyme [20, 23]. Since the ARS ribozyme is a de novo catalyst, in principle it has no limitation for the kinds of substrates used, i.e., it can be used with any tRNA and nonnatural amino acid. Thus, we have conceived this ribozyme system as a novel tool for the synthesis of engineered suppressor tRNAs charged with nonnatural amino acids. Although our original selection of catalytic precursor tRNA was designed to enrich active RNA sequences that aminoacylate a suppressor tRNA (referred to as otRNA; Figure 1B), the tRNA sequence in the selected clone contained two point deletions and two point mutations [16]. In fact, the *trans*-acting ribozyme, r24 or r24mini (a truncated version of r24 that exhibits wild-type activity), could aminoacylate Phe onto the mutant otRNA (v1-tRNA, Figure 1B) approximately 5-fold faster than the original otRNA. Moreover, r24mini is unable to charge Phe efficiently on an engineered suppressor tRNA ($tRNA^{Asn}_{CCCG}$) that is derived from *E. coli* $tRNA^{Asn}$ (Figure 1C). Therefore, the r24-based catalytic system is limited to utilizing otRNA variants (H. Murakami, D. Kourouklis, and H. Suga, submitted).

We report herein a 45-nucleotide ribozyme that exhibits a wider range of activity toward tRNAs than r24mini. This ribozyme was generated by in vitro selection using a partially randomized r24mini that was conjugated with $tRNA^{Asn}_{CCCG}$, followed by systematic engineering of a consensus sequence found in the active clones. Moreover, we found that this new ribozyme could tolerate nonnatural side chains on the Phe substrate. As a result, this small ribozyme acts as a versatile catalyst for the synthesis of aminoacyl-tRNAs charged with Phe analogs. Thus, this new ribozyme system potentially provides a useful tool for nonnatural amino acid incorporation into proteins using cell-free translation systems [24–27].

Results

Pool Design

Our previous studies on the structure-function relationship of r24 determined the essential catalytic core of ribozyme in the vicinity of J2/3 and L3 [28, 29]. Based on chemical modification and NAIM (nucleotide analog interference mapping) data, we have proposed that U32–U35 and U40–U41 consist of the Phe binding site (Figure 1A). Moreover, chemical mapping together with

*Correspondence: hsuga@buffalo.edu
[2]Current address: Research Center for Advanced Science and Technology, University of Tokyo, 4-6-1 Komaba, Meguro-ku, Tokyo, 153-8904, Japan.
[3]Current address: Cancer Institute, Japanese Foundation for Cancer Research, 1-37-1 Kami-ikebukuro, Toshima-ku, Tokyo, 170-8455, Japan.

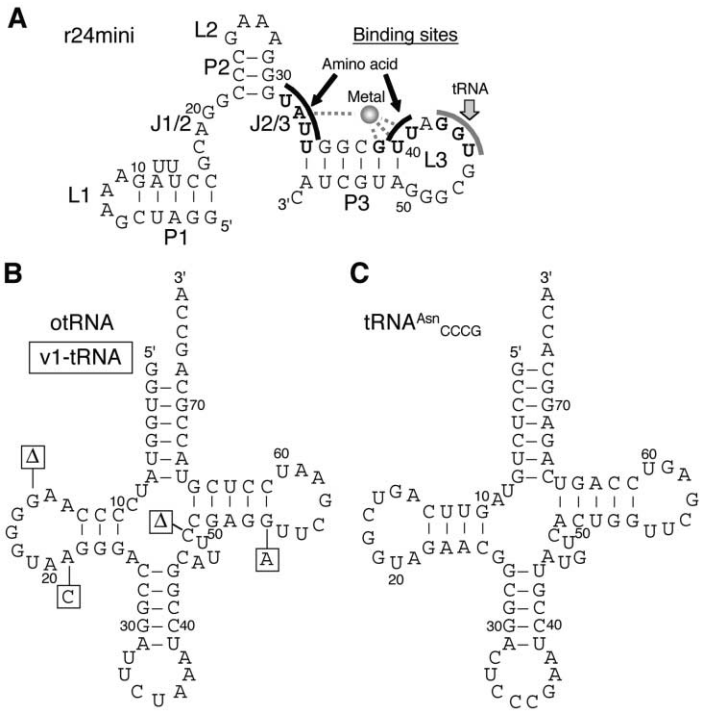

Figure 1. r24mini and tRNAs

(A) r24mini: The critical bases identified in previous studies are highlighted in bold with black lines (amino acid binding site), gray line (tRNA binding site), and gray dashed lines (metal binding site). The tRNA binding site (G43–U45) of r24mini forms base pairs with G_{73}–C_{75} of v1-tRNA.

(B) otRNA and v1-tRNA (rectangles). The rectangles indicate mutations and deletions (Δ) found in v1-tRNA. These mutations cause an increase in aminoacylation efficiency by r24mini.

(C) $tRNA^{Asn}_{CCCG}$: Bases in all tRNAs are numbered according to the tRNA numbering rule.

compensatory mutations corroborated the base-pairing interaction between G43–U45 and G/A/U_{73}–C_{75} (subscripted number refers to the number of tRNA bases). However, if only the above base-pairing interaction between the ribozyme and tRNA dictates binding, it cannot explain the observation that r24mini aminoacylates v1-tRNA more efficiently than otRNA [16] or $tRNA^{Asn}_{CCCG}$ [27, 30]. This instead suggests that the pair of r24mini and v1-tRNA may have interactions that do not exist in the other less active r24mini–tRNA pairs, and such interactions may contribute to increase in activity. Alternatively, r24mini somehow constrains its own structure that cannot adapt to other tRNA structures.

In order to evolve r24mini to ones that have higher activity toward other tRNAs, we decided to build RNA pools based on the r24mini sequence containing randomized bases in certain regions. The previously identified amino acid and tRNA binding sites were left intact (except for G39) to avoid a significant loss in activity. We also wished to search all possible sequence space and therefore decided to design pools with only a 19 nucleotide (nt) random sequence to the pool (its complexity is 2.8×10^{11}). Based on these considerations, we prepared two doped pools that have random sequences in different regions (Figure 2).

In pool 1 (Figure 2A), random bases were introduced at bases 12–19 and 46–56 (note that the base numbering was kept the same as r24mini for convenience of comparison, while the P1 stem was extended in order to facilitate annealing of the 5′ primer during PCR). The former random region was designed to address questions of whether the bulged U21 and U22 as well as bases at J1/2a play important roles in contributing to the activity. The latter region was designed to investigate whether sequences downstream of the tRNA binding site are able to increase activity. In pool 2 (Figure 2B), random bases were implemented into bases 36–39 and 46–56, including a 4-base insertion in L3 (50-*2*–50-*5*;

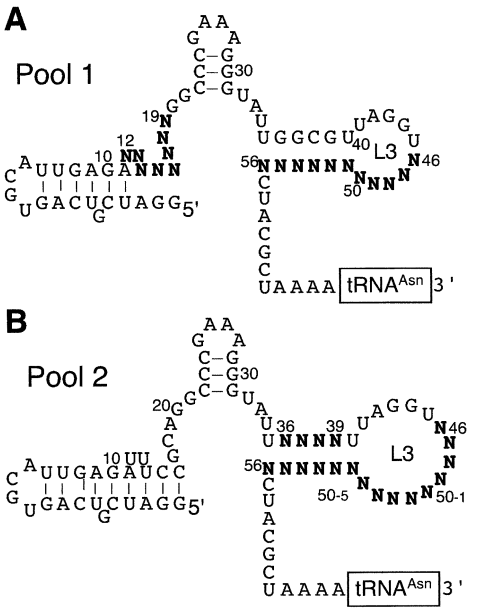

Figure 2. Pool Designs

(A) Pool 1: The introduced random bases are shown in N. The base numbering was kept as same as that of r24mini, while 9 nucleotides were inserted in the P1 stem in order to present enough base-pair interactions for 5′ primer annealing.

(B) Pool 2: This pool has an insertion of 4 bases into the 46–56 region, shown as 50-X (X = 2–5). Otherwise, the same design as in pool 1 was applied.

italicized numbers indicate the inserted bases). Since bases 36–39 in P3 were flanked between two essential regions of the amino acid binding site, randomizing this region was designed to examine the necessity of this particular sequence. Their counter bases in P3 (52–55) were also randomized to find alternate pairs in P3. To increase the likelihood that the selected *cis*-acting ribozymes can also function in *trans*, we designed a 10-base-long linker where the sequence was designed based on the sequence previously selected (6 bases) with four additional adenines. This linker was tested using the r24mini–linker–v1-tRNA prior to constructing the pool, and the wild-type activity with this construct was confirmed. Thus, we synthesized these two pools that were conjugated with $tRNA^{Asn}_{CCCG}$ via the 10-base linker.

Selection from the Doped Pools

The two pools were mixed and applied to selection with Biotin-Phe-CME as the substrate using the same procedures as previously reported [16]. Activity became apparent after four rounds of selection (data not shown), and the selection was continued for two more rounds at a shorter incubation time (30 min → 10 min) to produce a more active population. After cloning of the active population, 18 clones were arbitrarily chosen to screen for self-aminoacylation activity, and 16 active clones were identified. These clones were sequenced and aligned (see Supplemental Data at http://www.chembiol.com/cgi/content/full/10/7/655/DC1).

We found that only two clones originated from pool 1, and the remaining fourteen clones were from pool 2, suggesting that active sequences were more abundant in pool 2. Between the two active clones in pool 1, the wild-type sequence was partially recovered in the 12–19 region. Positions 12–14 were not conserved, while C15–A19 were the wild-type sequence, indicating the importance of this particular sequence for activity. In contrast, it was surprising to find that the 46–56 region did not yield a wild-type nor any similar sequence among two clones.

Among the fourteen clones isolated from pool 2, we found that the 36–39 region was completely conserved. This strongly argues that this particular sequence is essential for activity. In contrast, the 46–56 region had neither the wild-type nor a consensus sequence. This was consistent with the observation in the clones selected from pool 1. These observations led us to hypothesize that this region might be unnecessary to form not only the P3 stem but also even any structures.

Engineering Truncated Ribozymes

To test the above hypothesis, we first constructed a truncated ribozyme based on the consensus sequence found in pool 2 where the entire sequence downstream of the tRNA binding site (beyond U45) was deleted. This truncated ribozyme showed virtually identical activity as the clones isolated from pool 2 (data not shown), supporting the hypothesis. This ribozyme was further truncated by shortening the P1 stem-like r24mini, and a series of mutants (Fx series in Figure 3A; Fx was named after Flexizyme) were constructed varying the length of the complementary sequence to the $tRNA^{Asn}_{CCCG}$ 3′ end. Using this series of mutants, we wanted to address the importance of the strength of the base-pair interaction between the ribozyme and the $tRNA^{Asn}_{CCCG}$.

The initial rates of aminoacyl-$tRNA^{Asn}_{CCCG}$ formation were analyzed for all of the constructs by streptavidin (SAv)-dependent gel-shift assay (Figure 3B). Fx3, which has 3 bases (G43–U45) complementary to the tRNA 3′ end (A_{73}–C_{75}), exhibited the highest activity among the tested mutants (Figure 3B). The observed rate of Fx3 was 69 nM/min, which has 29-fold higher activity than r24mini (2.4 nM/min). Shortening the complementary bases to 2 (Fx2) reduced the observed rate significantly (5.8 nM/min), indicating the significance of the 3-base-pair interaction. On the other hand, increasing the complementary bases to 4 (Fx4) afforded a mild reduction in activity (52 nM/min), whereas increasing them to 5 (Fx5) decreased the observed rate further (21 nM/min). These results suggest that extension of the base-pairing interaction between the 3′ end of the ribozyme and the tRNA acceptor stem does not contribute to increasing activity, most likely because the bases added to the 3′ end of ribozyme cannot effectively invade the tRNA acceptor stem. Rather, it acts as a negative factor that interferes with the essential base-pair interaction of G43–U45 with A_{73}–C_{75}.

We also analyzed the end point of aminoacyl-tRNA product (Figure 3C). Since the Flexizyme constructs differ only in a few bases at the 3′ end, we expect that all the constructs fold similarly and hence display a similar end point. In fact, Fx3 and Fx4 constructs gave the same end point. Although we could not actually observe the end points for Fx2 and Fx5 in a 90 min incubation period due to their slow reactive rate, their end points could be extrapolated to be nearly the same as the other two constructs. This suggests that the observed initial rates of the tRNA aminoacylation shown in Figure 3B most likely reflect the activity of each construct. It should be noted that we could not see greater than 50% aminoacylated tRNA in any experiment when $tRNA^{Asn}_{CCCG}$ was the substrate. This is because the active fraction of $tRNA^{Asn}_{CCCG}$ for accepting the aminoacyl group is less than 50%, due to the heterogeneity of the 3′ end and possibly misfolding of the tRNA structure. This was supported by the observation that when different tRNAs were used, the end points were varied depending upon the tRNA construct (data not shown). Moreover, this was also supported by the fact that addition of an excess amount of ribozyme did not change the yield of aminoacylated $tRNA^{Asn}_{CCCG}$ (data not shown).

Kinetic Parameters of Fx3

Having the optimized ribozyme (Fx3) for aminoacylation of $tRNA^{Asn}_{CCCG}$, we next attempted to determine its kinetic parameters. Prior to accessing such values, we first needed to know K_M of Fx3 for the amino acid substrate in order to fix one variable. We took advantage of the corresponding *cis*-acting system to investigate the K_M for Biotin-Phe-CME. The *cis*-acting construct was prepared by directly connecting the 5′ end of tRNA to the

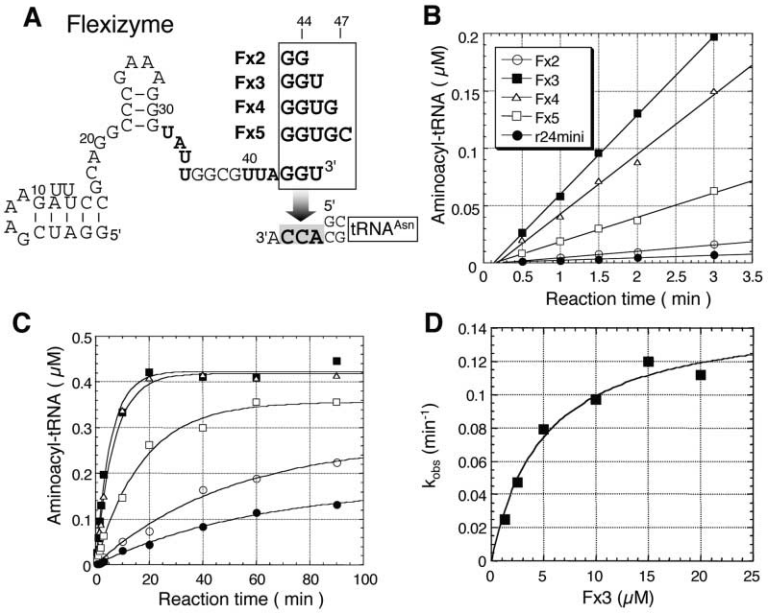

Figure 3. Flexizymes and Their Aminoacylation Efficiencies toward $tRNA^{Asn}_{CCCG}$

(A) A series of Flexizyme derivatives (Fx2–5). The critical bases found in the studies on r24mini are highlighted in bold (see also Figure 1A). The 3′ ends of those Flexizymes, which are complementary to the 3′ end of tRNA (A_{73}–C_{75}), are manipulated in each construct to form additional base pairs (Fx4 and Fx5) or lack one base pair (Fx2) as shown.

(B) Comparison of the initial rates between Flexizymes (Fx2–5) and r24mini. Data obtained in 0.5–3 min were fit to a linear plot. The observed rates were 5.8, 69, 52, and 21 nM/min for Fx2–5, respectively, and 2.4 nM/min for r24mini.

(C) Comparison of the ribozyme activities in 0.5–90 min. Data were fit to the first-order kinetic equation, which gave virtually the same values as those derived from the linear plots. In these experiments, reactions were carried out in the presence of 1 μM $tRNA^{Asn}_{CCCG}$, 2 μM ribozyme, and incubated with 5 mM Biotin-Phe-CME at 25°C, and amounts of the aminoacyl-tRNA product were determined by SAv gel-shift assay.

(D) Single turnover kinetics of Fx3. Reactions were performed with a fixed concentration of $tRNA^{Asn}_{CCCG}$ (0.1 μM) with various concentrations of Fx3 (1.25–20 μM). The data were fitted with the Michaelis-Menten equation, giving K_M^{app} = 5.0 μM and k_{cat} = 0.15 min^{-1}.

3′ end of Fx3 (see Figure 3A), in which the tRNA binding site of Fx3 should be always occupied with tRNA. Using this *cis*-acting Fx3, the initial rate for the aminoacylated product was measured in the presence of 1–6 mM Biotin-Phe-CME. The observed rate constants linearly increased in this range (0.024–0.11 min^{-1}; data not shown); unfortunately, due to the limited solubility of the amino acid substrate in aqueous buffers, concentrations more than 6 mM could not examined. This is an interesting contrast to our previous observation that the original r24-tRNA *cis*-acting system (pre-24) shows a saturation behavior with K_M = 2.8 mM and k_{cat} = 0.13 min^{-1} (note that 100 mM Mg^{2+} was used for both studies) [16]. Although more detailed investigations are necessary to understand the exact reason that causes the observed difference between these two *cis*-acting systems, it is clear that Fx3 has lost affinity somewhat toward the amino acid substrate. This may be attributed to the fact that the putative amino acid binding site in Fx3 resides in the single-stranded region, whereas that in r24 resides in the more rigidly structured region involving the P3 stem. Most importantly, the observed rate constant of Fx3 at 5 mM substrate is nearly identical to that of r24 at the same substrate concentration. We therefore attempted to access the apparent K_M (defined as K_M^{app}) value for tRNA using 5 mM Biotin-Phe-CME. Although this K_M^{app} is not actual K_M, it should evaluate the kinetic significance in the Fx3 *trans*-acting system.

To measure the single turnover rate of Fx3, the kinetic experiments were performed in the presence of various excess concentrations of Fx3 (1.25–20 μM) over a fixed concentration of $tRNA^{Asn}_{CCCG}$ (0.1 μM). The data fit to a typical single site saturation curve according to the Michaelis-Menten equation, giving a K_M^{app} of 5.0 μM and a k_{cat} of 0.15 min^{-1} (Figure 3D). Although the determined k_{cat} value is not a true k_{cat} value, due to incomplete saturation of the amino acid binding site with the amino acid substrate, the k_{cat} value (0.15 min^{-1}) is the same as that observed for pre-24 under the same conditions. We thus believe that the real k_{cat} is not far different from the k_{cat} determined herein (presumably it would be slightly higher than the observed value if the tRNA binding site is saturated). Based on the above result, we assume that the difference in activity observed for Flexizyme mutants (Fx2–Fx5) observed in Figure 3B is probably due to the difference in K_M^{app} values rather than k_{cat}.

Multiple Turnover Ability

Since Fx3 bears a rather high K_M^{app} for tRNA, we thought that this ribozyme might be able to display multiple turnover activity. We therefore investigated this possibility by designing a series of experiments under multiple turnover conditions using a constant tRNA concentration (5 μM) and three concentrations of Fx3 at 0.02, 0.1, and 0.5 μM. The apparent rate was faster when a higher concentration of Fx3 was used (Figure 4A), but higher numbers of turnovers per ribozyme are observed at a lower concentration of Fx3 (Figure 4B); 0.02 μM Fx3 displayed 14 turnovers, whereas 0.1 and 0.5 μM Fx3 showed only 6 and 2 turnovers, respectively. It was interesting to see that the yield of aminoacyl-tRNA completely plateaued after the formation of 1 μM of aminoacyl-tRNA when 0.5 μM Fx3 was used. This suggests that turnover is strongly inhibited by the aminoacyl-tRNA product. Although more quantitative discussion awaits further investigations to determine the thermodynamic and kinetic parameters in detail, this strong product inhibition seems to limit the turnover activity of Fx3. In contrast to the observation for Fx3, r24mini completely lacks multiple turnover ability (Figures 4A and 4B).

Aminoacylation of Various tRNAs

The structure of Fx3 suggested that the base-pair interaction between G43–U45 and A_{73}–C_{75} might be the only

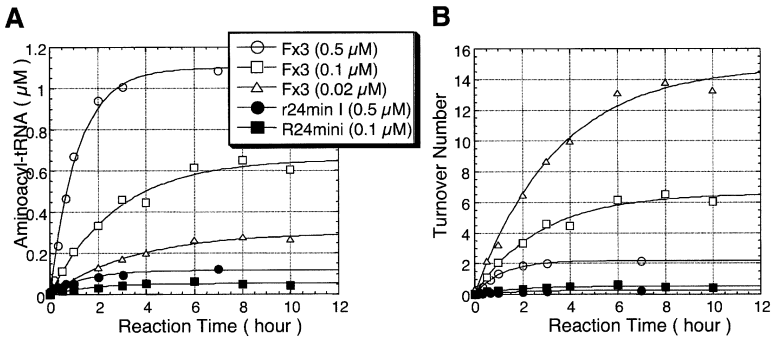

Figure 4. Multiple Turnover Abilities of Fx3 and r24mini

(A) Comparison of the ribozyme activities under multiple turnover conditions. $tRNA^{Asn}_{CCCG}$ and v1-tRNA were used as a tRNA substrate for Fx3 and r24mini, respectively.

(B) Numbers of turnovers per ribozyme. The concentrations of aminoacyl-tRNA observed in (A) were divided by each ribozyme concentration. Reactions were carried out in the presence of 5 μM tRNA ($tRNA^{Asn}_{CCCG}$ for Fx3, v1-tRNA for r24mini) and 0.02, 0.1, or 0.5 μM Fx3 or 0.5 or 0.1 μM r24mini and incubated with 5 mM Biotin-Phe-CME at 25°C. Due to the low activity of r24mini, reliable data using 0.02 μM r24mini could not be generated.

determinant for interaction between Fx3 and $tRNA^{Asn}_{CCCG}$. This predicts that Fx3 may be able to aminoacylate various tRNAs with comparable efficiencies as long as the number of the complementary bases is kept the same. To test the idea, we prepared two naturally occurring tRNAs ($tRNA^{fMet}$ and $tRNA^{Phe}$) and three distinct artificial tRNAs (otRNA, v1-tRNA, and $tRNA^{Asn}_{CCCG}$). We also prepared three $tRNA^{Asn}_{CCCG}$ mutants containing different bases at position 73 (N_{73}, discriminator base) to see the importance of recognition of this base by U45 in Fx3.

We investigated the aminoacylation yield of each tRNA after 3 min incubation, corresponding to the initial rate for the tRNA (Figure 5A). The two natural tRNAs, $tRNA^{Asn(A)}_{CCCG}$ and $tRNA^{Asn(G)}_{CCCG}$, both of which have A or G of the discriminator base, were aminoacylated with comparable initial rates by Fx3. On the other hand, $tRNA^{Asn(C)}_{CCCG}$ and $tRNA^{Asn(U)}_{CCCG}$, both of which form a mispair with 45U in Fx3, were not aminoacylated as fast as the other tRNAs. In particular, $tRNA^{Asn(C)}_{CCCG}$ was aminoacylated more than 5-fold slower than $tRNA^{Asn(A)}_{CCCG}$. These results suggest that the difference in activities of the $tRNA^{Asn}_{CCCG}$ mutants is attributable to the recognition of the discriminator base by Fx3, most likely due to an increase in K_M^{app} for the mispairing tRNAs.

On the other hand, r24mini aminoacylates tRNAs with much poorer rates than Fx3 (Figure 5A). The yields of most tRNAs were less than 2%, and the only tRNA that showed a decent yield (9%) was v1-tRNA. Thus, r24mini has greater preference toward v1-tRNA, although the activity is considerably poorer than the activities observed in the series of experiments with Fx3. Although the specific molecular interactions occurring in the r24mini–v1-tRNA pair are still unknown, it is clear that the loss of such specific interactions in Fx3 has made it a better catalyst.

The above observation led us to test a simpler tRNA analog, minihelix RNA (Figure 5B), as a substrate for aminoacylation by Fx3. Our previous studies on r24mini revealed that it could aminoacylate a minihelix RNA consisting of the acceptor and T stems of v1-tRNA, but the activity is poorer than v1-tRNA due to loss of the unknown interactions. Since Fx3 interacts with tRNA

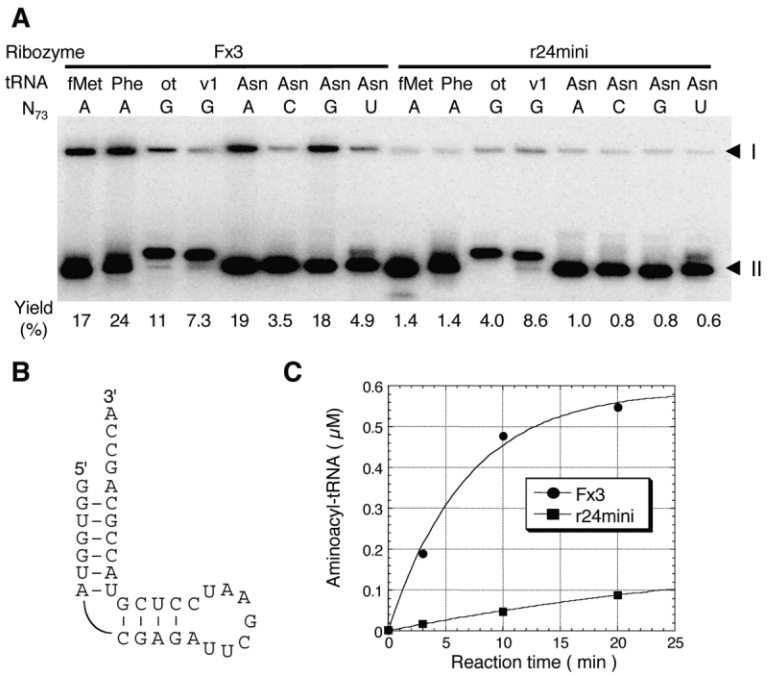

Figure 5. Aminoacylation Activities of Fx3 and r24mini toward Various tRNAs and a Minihelix RNA

(A) Aminoacylation activities Fx3 and r24mini toward various tRNAs. Reactions were carried out in the presence of 1 μM tRNA and 2 μM Fx3 or r24mini and incubated with 5 mM Biotin-Phe-CME at 25°C for 3 min. fMet, $tRNA^{f\text{-}Met}$; Phe, $tRNA^{Phe}$; v1, v1-tRNA; ot, otRNA; Asn, $tRNA^{Asn}$; N_{73}, discriminator base of tRNA; I, aminoacyl-tRNA complexed with SAv; II, unreacted tRNA. The yield was determined by I /(I + II).

(B) Secondary structure of the minihelix RNA derived from v1-tRNA.

(C) Comparison of the activities between Fx3 and r24mini. Reactions were carried out in presence of 1 μM minihelix RNA and 2 μM Fx3 or r24mini and incubated with 5 mM Biotin-Phe-CME at 25°C.

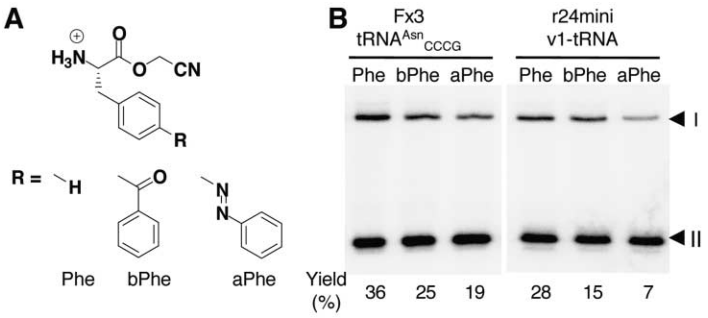

Figure 6. Aminoacylation of tRNA with Phe Analogs by Fx3 and r24mini

(A) Chemical structure of Phe and its analogs activated by cyanomethyl ester. Phe, phenylalanine; bPhe, *p*-benzoyl-phenylalanine; aPhe, *p*-azophenyl-phenylalanine.

(B) Comparison of aminoacylation efficiencies of Fx3 and r24mini with Phe analogs. Reactions were carried out in the presence of 1 μM tRNA and 2 μM Fx3 or r24mini and incubated with 10 mM Phe or Phe analogs on ice for 2 hr. Note that because of instability of the α-NH_2 Phe substrates against hydrolysis, the reactions were carried out on ice instead of 25°C. To separate the aminoacyl-tRNA from unreacted tRNA, post-biotinylation of the product using biotin sulfo-NHS ester was performed in order to run the SAv-dependent gel-shift assay. This method was previously shown to selectively biotinylate the α-NH_2 group [16, 20, 36]. Abbreviations are the same as in Figure 5A.

only through the 3 base pairs, it should be able to aminoacylate the minihelix RNA as effectively as other tRNAs tested. Indeed, Fx3 aminoacylates the minihelix RNA with a comparable rate to tRNA$^{Asn}_{CCCG}$ (Figure 5C). We also observed that the end point slightly increased compared with tRNA$^{Asn}_{CCCG}$, presumably due to increased fraction of correct folding. Thus, these experiments prove that the molecular interaction between Fx3 and tRNA is only the 3 base pairs.

tRNA Aminoacylation with Nonnatural Amino Acids

We have previously reported that r24mini is able to charge Phe and Tyr (with α-N-biotinylated group as well as free α-NH_2 group) onto v1-tRNA. More recently, we have found that it also tolerates some Phe analogs with reduced efficiencies (vide infra). Since Fx3 is superior to r24mini as a tRNA aminoacylation catalyst, we wondered whether it could exhibit higher activity toward the Phe analogs. To test this, we chose two Phe analogs, *p*-benzoyl-phenyalanine (bPhe) and *p*-azophenyl-phenylalanine (aPhe), both of which have a large group at the para substitution of the aromatic side chain (Figure 6A). The side chains in the aforementioned Phe analogs contain photo-crosslinkable and photo-switchable groups, respectively. It should be noted that in this series of experiments we used those with the free α-NH_2 group rather than the *N*-biotinyl group, since the ultimate goal of this program is to generate elongator aminoacyl-tRNAs.

As expected, Fx3 exhibits greater activities toward both Phe analogs than r24mini (Figure 6B). Most importantly, we have already confirmed the orthogonality of tRNA$^{Asn}_{CCCG}$ (which is inert to *E. coli* endogenous ARSs) and effective suppression of the programmed frameshift mutation on mRNA using a cell-free translation system (H. Murakami, D. Kourouklis, and H. Suga, submitted), so that the ability of Fx3 to charge tRNA$^{Asn}_{CCCG}$ with the Phe analogs will provide a new tool for nonnatural amino acid incorporation into proteins.

Discussion

In vitro evolution of ARS ribozymes using a structural scaffold of r24mini successfully yielded a new truncated ribozyme, referred to as Flexizyme (Fx3), that shows greater activity toward tRNA$^{Asn}_{CCCG}$ than r24mini. It was surprising to find that the solution for enhancing the activity toward tRNA$^{Asn}_{CCCG}$ was very simple: extra interactions that uniquely exist in the parent ribozyme-tRNA pair were removed, dictating the essential interactions into only 3 base pairs, Fx3 G43–U45 and tRNA$^{Asn}_{CCCG}$ A_{73}–C_{75}. This resulted in loss of tRNA selectivity of Fx3, but enabled Fx3 to charge Phe onto various tRNAs with much higher activity than r24mini.

It should be noted that the essential 3-base-pair interaction is present in not only the new ribozyme-tRNA pair (Fx3–tRNA$^{Asn}_{CCCG}$) but also the parent pair (r24mini–v1-tRNA). Then how did removal of the unknown interactions existing in the parent pair result in the enhancement of activity? We suggest that the flexible single-stranded region of the catalytic core in Fx3 may play an important role. It should be noted that our previous studies on the parent ribozyme system using nuclease/chemical mapping and NAIM supported the single-stranded structures in G17–G21 and U32–U35 as well as the formation of the P3 stem [28]. Removal of the nonessential sequence present in the parts of L3 and P3 gave Fx3 a long single- stranded region beyond U45. In particular, U35–G39, which originally forms the P3 stem, became single stranded. However, all critical bases for activity, which include the amino acid binding site, tRNA binding site, and metal binding site (see bold bases in Figure 3A), were retained in Fx3. Thus, it is clear that even though the core sequence resides in the single-stranded region in Fx3, the catalytic site is properly formed. This flexible structure is more suited for adapting to various tRNAs than the structurally rigid r24mini, where some parts of the essential core sequence are present in the stem, loop, and junction. We thus propose that the increase in activity toward various tRNAs is realized by the "induced fit"-like property of Fx3. Although a large portion of the secondary structure of Fx3 consists of single-stranded regions, upon binding to tRNA it may be able to fold properly in the tertiary space and adapt to the 3′ end of any tRNAs. Although this is our current working hypothesis, we plan on conducting more detailed experiments in order to understand the dynamic change in the core structure occurring in Fx3.

Restricting the interaction between Fx3 and tRNA to the essential 3 base pairs also seemed to weaken their affinity. This enabled Fx3 to display a modest yet multiple turnover activity that could not be observed in

r24mini at all. The multiple turnover ability seems to be limited by strong product inhibition. This can be attributed to the higher affinity of aminoacyl-tRNA product to Fx3 than tRNA, due to the additional complex stability gained from the ribozyme–amino acid interaction. This would be the intrinsic limitation of this ribozyme system for multiple turnovers. However, it would also be a unique feature that allows us to devise a solid-phase catalytic system, where the ribozyme is immobilized on a resin, and this ribozyme resin can be used to generate and isolate aminoacyl-tRNAs with great facility, as previously reported [23]. The lack of preference toward various tRNAs is particularly attractive to generate various mischarged tRNAs. This ribozyme system can be used, for instance, to generate mischarged tRNAs, which could provide an excellent tool for studies of aminoacyl-tRNA associated with macromolecules such as EF-Tu [31–33]. Obviously, this artificial genetic coding system can also be used to incorporate Phe analogs into proteins. Such applications using this Flexizyme system are underway in our laboratory.

Significance

Reevolution of an ARS ribozyme yielded a short 45 nt ribozyme, called Flexizyme, consisting of a long flexible single-stranded sequence. The catalytic core in the Flexizyme resides in this single-stranded region, but upon forming a complex with tRNA it constitutes the active structure to catalyze the tRNA aminoacylation. This flexibility toward various tRNAs and Phe analogs will allow us to use this de novo aminoacylation system in many applications.

Experimental Procedures

Pool Construction

The following oligonucleotides containing random sequence (N) were chemically synthesized: P1 (5′-GGATCGTCAG TGCATTGAGA-N8-GGCCCGAAAG GGTATTGGCG TTAGGT-N11-CTACGCTAA AA GCCTCTGTA GTTCAGTCGG T-3′), P2 (5′-GGATCGTCAG TGCAT TGAGA TTTCCGCAGG CCCGAAAGGG TATT-N4-TTAGGT-N15-CTA CGCTAA AAGCCTCTGT AGTTCAGTCG GT-3′), T7 (5′-GGTAACA CGC ATATG*TAATA CGACTCACTA TAG*GATCGTC AGTGCATTGA GA-3′; T7 promoter sequence is italicized), TR (5′-TGGTGCCTCT GACTGGACTC GAACCAGTGA CATACGGATT CGGGAGTCCG CCG TTCTACC GACTGAACTA CAGAGGC-3′), and TR3 (5′-TGGTGCC TCT GACTGGACTC-3′). A 200 μl scale of *Taq* DNA polymerase extension using the DNA templates of P1 (20 pmol) or P2 (20 pmol) and TR (20 pmol) was performed with a thermocycle at 95°C for 2 min, 50°C for 2 min, and 72°C for 10 min. The resulting full-length product was then diluted to 1 ml and subjected to 6 cycles of PCR amplification (95°C for 1 min, 55°C for 1 min, and 72°C for 1 min) in the presence of the T7 and TR3 primers. After phenol-chloroform extraction and ethanol precipitation, each PCR product was quantified, and 10 pmol of each DNA pool was mixed. This mixture of the DNA pools was in vitro transcribed in the presence of [α-^{32}P]UTP, and the RNA transcripts were purified by 6% denaturing PAGE.

Substrates

Biotin-Phe-CME (α-*N*-biotinyl-phenylalanine cyanomethyl ester) and Phe-CME (phenylalanine cyanomethyl ester) were synthesized using the same procedure as previously described [16, 34]. bPhe-CME (*p*-benzoyl-phenyalanine cyanomethyl ester) was synthesized from the *N*-Boc amino acids by using the same procedure as Phe-CME. aPhe-CME (*p*-azophenyl-phenylalanine cyanomethyl ester) was synthesized from *p*-amino-phenylalanine according to the literature procedures [35].

Selection

Selection reactions were carried out under the following conditions: 50 μl (100 μl for the first round) of 1 μM RNA pool, 2.5 mM Biotin-Phe-CME in EK buffer [50 mM N-(2-hydroxyethyl)piperazine-N′-(3-propanesulfonic acid); EPPS, 12.5 mM KCl (pH 7.5)], 100 mM $MgCl_2$, and 5% ethanol. The procedure was as follows: the pool RNA was heated at 95°C for 3 min and cooled to 25°C over 5 min. $MgCl_2$ (100 mM final concentration) was added, followed by a 5 min equilibration. The reaction was initiated by addition of Biotin-Phe-CME in ethanol:water (1:1) and incubated for 30 min (10 min for fifth and sixth rounds). The reaction was stopped by addition of 2 volumes of ethanol, and the RNA was precipitated. The RNA pellet was rinsed with 70% ethanol three times, dissolved into EK2 buffer (50 mM EPPS, 500 mM KCl [pH 7.5]), and then 4 units of RNase inhibitor and 4 μl of streptavidin(SAv)-agarose were added. The mixture was incubated for 30 min at 4°C, then the resin was washed six times with 100 μl of EK2 buffer, three times with 100 μl of 4 M urea, and two times with 100 μl of water. RNAs that nonspecifically bind to the agarose resin were removed by heating the resin for 30 s at 95°C in 100 μl of 20 mM EPPS (pH 7.0) followed by washing with 100 μl of water. The resin was added to a 10 μl solution of 1 μM of TR primer, 125 μM dNTPs, 50 mM Tris-HCl (pH 8.3), 75 mM KCl, 3 mM $MgCl_2$, 10 mM dithiothreitol, 0.2 μg of SAv, and 50 units of MMLV reverse transcriptase (Promega, WI). Then the whole reaction mixture was incubated for 1 hr at 42°C. A PCR buffer containing the 5′ and 3′ primers and *Taq* DNA polymerase was added to the whole RT mixture and subjected to theremocycling to amplify the cDNA sequence. The amplification was confirmed by electrophoresis on 3% agarose, and the dsDNAs were isolated using standard protocols. In the sixth round of selection, the dsDNAs were cloned into a pGEM-T vector (Promega), and the cloned plasmids were harvested for sequencing using standard protocols.

Preparation of Ribozymes and tRNAs

The cDNA sequence of each ribozyme (Fx2–5, Figure 3) was chemically synthesized and purified by 6% denaturing PAGE. This cDNA was annealed with the 5′ primer (5′-GGTAACACGC ATATG*TAATA CGACTCACTA TA*GGATCGAA AGATTTCCGC-3′) and extended by *Taq* DNA polymerase. The resulting dsDNA was transcribed in vitro using T7 RNA polymerase. The transcript was purified on 10% denaturing PAGE and isolated by elution from the sliced gel(s) using 0.3 M NaCl followed by ethanol precipitation. The tRNA dsDNA template was prepared from the corresponding synthetic cDNA by PCR in the presence of the corresponding 5′ and 3′ primer oligonucleotides and transcribed in vitro in the presence of 7.5 mM GMP, 3.75 mM of each NTPs, and [α-^{32}P]UTP or [α-^{32}P]GTP to prepare the body-radiolabeled 5′-P-tRNA molecule (Figures 1A and 1B).

Aminoacylation Assay

The *trans*-aminoacylation activities were assayed under the following condition: 5 mM Biotin-Phe-CME in EK buffer, 500 mM $MgCl_2$ and 15% DMSO (dimethyl sulfoxide) in the presence of 1 μM tRNA, 2 μM ribozyme. Alternatively, 0.1 μM tRNA and 1.25–20 μM ribozyme (Fx3) were used for determination of K_M^{app} toward tRNA, or 5 μM tRNA and 0.02–0.5 μM ribozymes were used for multiple turnover analysis. The procedure was as follows: the tRNA and ribozyme were dissolved into EK buffer independently, heated at 95°C for 3 min, and cooled to 25°C over 5 min. $MgCl_2$ (500 mM for final concentration) was added, followed by a 5 min equilibration. The two solutions were then mixed and incubated for 5 min at 25°C. The reaction was initiated by addition of Biotin-Phe-CME in DMSO and incubated at 25°C. At each time point, an aliquot of the reaction was ethanol precipitated. The pellet was dissolved into 1 μl of water, and then 4 μl of the loading buffer (0.62 mg/ml SAv, 50 mM EDTA, 33 mM piperazine-N′N-bis-[2-ethanesulfonic acid] [pH 6.1], 6 M urea) was added to the solution. The solution was heated for 30 s at 95°C, and then cooled to 25°C. The resulting solution was analyzed by 8% denaturing PAGE running in a cold room in order to keep the gel temperature $<$20°C. Under these conditions, the SAv-biotin

complex is stable to retard the aminoacyl-tRNA band, but the RNA structure is denatured.

The *trans*-aminoacylation activities in the presence of Phe-CME, bPhe-CME, and aPhe-CME were assayed under the following conditions: 10 mM amino acid substrates in EK buffer (pH 7.0), 500 mM $MgCl_2$ (in the case of bPhe-CME, 5% ethanol was added to avoid its precipitation) in the presence of 1 μM tRNA, 2 μM ribozyme. The remaining procedure is similar to that for Biotin-Phe-CME, except for the reaction temperature (on ice instead of 25°C), and the post-biotinylation [16, 20, 36] was carried out according to the following procedure. After 2 hr incubation on ice, the reaction was stopped by addition of 2 volumes of ethanol, and then the RNA was precipitated. The pellet was dissolved in 2.5 μl of EPPS (0.1 M, pH 5.9), 20 mM biotin-3-sulfo-*N*-hydroxylsuccinimide ester at 0°C, and then 0.86 μl of EPPS-KOH (0.3 M, pH 9.1) was added to this solution, which brought the pH to 8.0. After 1 hr, the reaction was terminated by ethanol precipitation. The pellet was dissolved in water and analyzed by SAv-dependent gel-shift assay as described above.

Acknowledgments

We thank D. Kourouklis and K. Ramaswamy for synthesizing amino acid substrates and proofreading. H. Murakami and H. Saito acknowledge JSPS Research Fellowship for Young Scientists. This work was supported by the National Institutes of Health (GM59159) and a Human Frontier Science Program awarded to H. Suga.

Received: May 1, 2003
Revised: May 31, 2003
Accepted: June 4, 2003
Published: July 18, 2003

References

1. Cech, T.R. (2000). Structural biology. The ribosome is a ribozyme. Science *289*, 878–879.
2. Yusupov, M.M., Yusupova, G.Z., Baucom, A., Lieberman, K., Earnest, T.N., Cate, J.H., and Noller, H.F. (2001). Crystal structure of the ribosome at 5.5 A resolution. Science *292*, 883–896.
3. Ban, N., Nissen, P., Hansen, J., Moore, P.B., and Steitz, T.A. (2000). The complete atomic structure of the large ribosomal subunit at 2.4 A resolution. Science *289*, 905–920.
4. Nissen, P., Hansen, J., Ban, N., Moore, P.B., and Steitz, T.A. (2000). The structural basis of ribosome activity in peptide bond synthesis. Science *289*, 920–930.
5. Gilbert, W. (1986). The RNA world. Nature *319*, 618.
6. Illangasekare, M., Sanchez, G., Nickles, T., and Yarus, M. (1995). Aminoacyl-RNA synthesis catalyzed by an RNA. Science *267*, 643–647.
7. Lohse, P.A., and Szostak, J.W. (1996). Ribozyme-catalysed amino-acid transfer reactions. Nature *381*, 442–444.
8. Tarasow, T.M., Tarasow, S.L., and Eaton, B.E. (1997). RNA-catalysed carbon-carbon bond formation. Nature *389*, 54–57.
9. Zhang, B., and Cech, T.R. (1997). Peptide bond formation by in vitro selected ribozymes. Nature *390*, 96–100.
10. Unrau, P.J., and Bartel, D.P. (1998). RNA-catalysed nucleotide synthesis. Nature *395*, 260–263.
11. Kumar, R.K., and Yarus, M. (2001). RNA-catalyzed amino acid activation. Biochemistry *40*, 6998–7004.
12. Johnston, W.K., Unrau, P.J., Lawrence, M.S., Glasner, M.E., and Bartel, D.P. (2001). RNA-catalyzed RNA polymerization: accurate and general RNA-templated primer extension. Science *292*, 1319–1325.
13. Lee, N., Bessho, Y., Wei, K., Szostak, J.W., and Suga, H. (2000). Ribozyme-catalyzed tRNA aminoacylation. Nat. Struct. Biol. *7*, 28–33.
14. Joyce, G.F. (2002). The antiquity of RNA-based evolution. Nature *418*, 214–221.
15. McGinness, K.E., and Joyce, G.F. (2002). RNA-catalyzed RNA ligation on an external RNA template. Chem. Biol. *9*, 297–307.
16. Saito, H., Kourouklis, D., and Suga, H. (2001). An in vitro evolved precursor tRNA with aminoacylation activity. EMBO J. *20*, 1797–1806.
17. Schimmel, P., and Kelley, S.O. (2000). Exiting an RNA world. Nat. Struct. Biol. *7*, 5–7.
18. Yarus, M. (1999). Boundaries for an RNA world. Curr. Opin. Chem. Biol. *3*, 260–267.
19. Lee, N., and Suga, H. (2001). A minihelix-loop RNA acts as a trans-aminoacylation catalyst. RNA *7*, 1043–1051.
20. Bessho, Y., Hodgson, D.R., and Suga, H. (2002). A tRNA aminoacylation system for non-natural amino acids based on a programmable ribozyme. Nat. Biotechnol. *20*, 723–728.
21. Ramaswamy, K., Wei, K., and Suga, H. (2002). Minihelix-loop RNAs: minimal structures for aminoacylation catalysts. Nucleic Acids Res. *30*, 2162–2171.
22. Saito, H., and Suga, H. (2001). A ribozyme exclusively aminoacylates the 3′-hydroxyl group of the tRNA terminal adenosine. J. Am. Chem. Soc. *123*, 7178–7179.
23. Murakami, H., Bonzagni, N.J., and Suga, H. (2002). Aminoacyl-tRNA Synthesis by a Resin-Immobilized Ribozyme. J. Am. Chem. Soc. *124*, 6834–6835.
24. Heckler, T.G., Chang, L.H., Zama, Y., Naka, T., Chorghade, M.S., and Hecht, S.M. (1984). T4 RNA ligase mediated preparation of novel "chemically misacylated" $tRNA^{PheS}$. Biochemistry *23*, 1468–1473.
25. Noren, C.J., Anthony-Cahill, S.J., Griffith, M.C., and Schultz, P.G. (1989). A general method for site-specific incorporation of unnatural amino acids into proteins. Science *244*, 182–188.
26. Bain, J.D., Glabe, C.G., Dix, T.A., and Chamberlin, A.R. (1989). Biosynthetic site-specific incorporation of a non-natural amino acid in vitro a polypeptide. J. Am. Chem. Soc. *111*, 8013–8014.
27. Hohsaka, T., Ashizuka, Y., Murakami, H., and Sisido, M. (1996). Incorporation of nonnatural amino acids into streptavidin through in vitro frame-shift suppression. J. Am. Chem. Soc. *118*, 9778–9779.
28. Saito, H., Watanabe, K., and Suga, H. (2001). Concurrent molecular recognition of the amino acid and tRNA by a ribozyme. RNA *7*, 1867–1878.
29. Saito, H., and Suga, H. (2002). Outersphere and innersphere coordinated metal ions in an aminoacyl-tRNA synthetase ribozyme. Nucleic Acids Res. *30*, 5151–5159.
30. Cload, S.T., Liu, D.R., Froland, W.A., and Schultz, P.G. (1996). Development of improved tRNAs for in vitro biosynthesis of proteins containing unnatural amino acids. Chem. Biol. *3*, 1033–1038.
31. Pleiss, J.A., and Uhlenbeck, O.C. (2001). Identification of thermodynamically relevant interactions between EF-Tu and backbone elements of tRNA. J. Mol. Biol. *308*, 895–905.
32. LaRiviere, F.J., Wolfson, A.D., and Uhlenbeck, O.C. (2001). Uniform binding of aminoacyl-tRNAs to elongation factor Tu by thermodynamic compensation. Science *294*, 165–168.
33. Asahara, H., and Uhlenbeck, O.C. (2002). The tRNA specificity of Thermus thermophilus EF-Tu. Proc. Natl. Acad. Sci. USA *99*, 3499–3504.
34. Suga, H., Lohse, P.A., and Szostak, J.W. (1998). Structural and kinetic characterization of an acyl transferase ribozyme. J. Am. Chem. Soc. *120*, 1151–1156.
35. Goodman, M., and Kossoy, A. (1966). Conformational aspects of polypeptide structure. XIX. Azoaromatic side-chain effects. J. Am. Chem. Soc. *88*, 5010–5015.
36. Putz, J., Wientges, J., Sissler, M., Giege, R., Florentz, C., and Schwienhorst, A. (1997). Rapid selection of aminoacyl-tRNAs based on biotinylation of alpha-NH2 group of charged amino acids. Nucleic Acids Res. *25*, 1862–1863.